Genetica (2016) 144:523–533
DOI 10.1007/s10709-016-9920-3

Fine mapping and genetic association analysis of *Net2*, the causative D-genome locus of low temperature-induced hybrid necrosis in interspecific crosses between tetraploid wheat and *Aegilops tauschii*

Kouhei Sakaguchi[1] · Ryo Nishijima[1] · Julio Cesar Masaru Iehisa[1] · Shigeo Takumi[1]

Received: 7 May 2016 / Accepted: 2 August 2016 / Published online: 8 August 2016
© Springer International Publishing Switzerland 2016

Abstract Hybrid necrosis has been observed in many interspecific hybrids from crosses between tetraploid wheat and the wheat D-genome donor *Aegilops tauschii*. Type II necrosis is a kind of hybrid incompatibility that is specifically characterized by low-temperature induction and growth suppression. Two complementary genes, *Net1* on the AB genome and *Net2* on the D genome, putatively control type II necrosis in ABD triploids and synthetic hexaploid wheat. Toward map-based cloning of *Net2*, a fine map around the *Net2* region on 2DS was constructed in this study. Using the draft genome sequence of *Ae. tauschii* and the physical map of the barley genome, the *Net2* locus was mapped within a 0.6 cM interval between two closely linked markers. Although local chromosomal rearrangements were observed in the *Net2*-corresponding region between the barley/*Brachypodium* and *Ae. tauschii* genomes, the two closely linked markers were significantly associated with type II necrosis in *Ae. tauschii*. These results suggest that these markers will aid efficient selection of *Net2* non-carrier individuals from the *Ae. tauschii* population and intraspecific progeny, and could help with introgression of agriculturally important genes from *Ae. tauschii* to common wheat.

Keywords Allopolyploid evolution · Chromosome synteny · Hybrid incompatibility · Single nucleotide polymorphism · Wheat

Introduction

Common wheat (*Triticum aestivum* L.) is an allohexaploid species with an AABBDD genome, derived from interspecific crossing between cultivated tetraploid wheat (*Triticum turgidum* L., genome constitution AABB) and *Aegilops tauschii* Coss. (DD) (Matsuoka 2011). The allohexaploid speciation process can be artificially reproduced through interspecific crosses and the following formation of synthetic wheat hexaploids (Kihara and Lilienfeld 1949; Mujeeb-Kazi et al. 1996). The tetraploid wheat cultivar Langdon (Ldn) is an efficient female parent for production of synthetic wheat hexaploids (Matsuoka and Nasuda 2004), whereas many accessions of *Ae. tauschii* show abnormal growth in artificial hybrids (2n = 3x = 21, ABD genome) crossed into Ldn (Matsuoka et al. 2007; Mizuno et al. 2010). The growth abnormalities in ABD triploids have been proposed to occur due to epistatic interaction between the tetraploid AB and the *Ae. tauschii* D genomes (Nishikawa 1960, 1962). Thus, postzygotic reproductive barriers between tetraploid wheat and *Ae. tauschii* inhibit the normal production of synthetic wheat hexaploids, and make it difficult to use agriculturally important genes in the *Ae. tauschii* population for wheat breeding through wheat synthetics. Therefore, fine mapping of the causal genes for the growth abnormalities in ABD triploids is important for efficient introgression of *Ae. tauschii* alleles into the common wheat genome.

The growth abnormalities in the ABD triploids between Ldn and *Ae. tauschii* include hybrid chlorosis, severe

Electronic supplementary material The online version of this article (doi:10.1007/s10709-016-9920-3) contains supplementary material, which is available to authorized users.

✉ Shigeo Takumi
takumi@kobe-u.ac.jp

[1] Graduate School of Agricultural Science, Kobe University, Rokkodai 1-1, Nada-ku, Kobe 657-8501, Japan

growth abortion (SGA), and two types of hybrid necrosis (type II and type III) (Mizuno et al. 2010). Abnormal chloroplasts form in the mesophyll cells before the leaves yellow in the triploid plants showing hybrid chlorosis (Nakano et al. 2015). SGA is always lethal, because SGA-exhibiting ABD triploids cease development and growth after expansion of the second or third leaves (Nishikawa 1960; Hatano et al. 2012). Cell death occurs gradually beginning with older tissues in hybrid lines showing type III necrosis, whereas type II necrosis lines show a necrotic phenotype under low temperature conditions (Nishikawa 1960; Mizuno et al. 2011). In addition to necrotic symptoms, low temperature represses mitotic cell division in the shoot apices of hybrid plants displaying type II necrosis (Mizuno et al. 2011). Out of these growth abnormalities, type II necrosis, is induced in most of the *Ae. tauschii* accessions examined previously (Mizuno et al. 2010). The *Ae. tauschii* accessions resulting in type II necrosis were mainly from the eastern regions of the native range (≥60° longitude), predominantly from Afghanistan and Pakistan (Mizuno et al. 2010). The early-flowering accessions spread mainly in the eastern habitats of *Ae. tauschii* (Matsuoka et al. 2008), and the spike and spikelet morphology in the eastern habitats clearly differs from that in the western habitats (Matsuoka et al. 2009; Takumi et al. 2009). Since the birthplace of common wheat has been supposed to be restricted to a narrow distribution range within the western habitats (Tsunewaki 1966; Dvorak et al. 1998; Wang et al. 2013; Nishijima et al. 2014), the eastern habitat accessions that provide agriculturally useful genes are not represented in the D genome of common wheat (Kajimura et al. 2011; Jones et al. 2013). Thus, type II necrosis should be overcome to comprehensively use the eastern habitat accessions of *Ae. tauschii* for wheat breeding.

Dislike type I necrosis observed in crosses between common wheat cultivars, type II necrosis has not been reported in any intraspecific cross of the *Ae. tauschii* accessions. Causal genes for type I necrosis, *Ne1* and *Ne2*, were respectively located on chromosome arms of 5BL and 2BS (Tsunewaki 1960; Chu et al. 2006). *Ne2* was assumed to be a wheat leaf rust resistance gene *Lr13* (Zhang et al. 2016). The D-genome causal gene, *Net2*, for type II necrosis in ABD triploids and wheat synthetics was assigned to the short arm of chromosome 2D (Mizuno et al. 2011), whereas homoeologous relation between *Ne2* and *Net2* is still unknown. Another *Net* gene, *Net1*, complementary to *Net2*, is proposed to be in the AB genome of tetraploid wheat, but no information on its chromosome location has been reported (Takumi and Mizuno 2011). At least one wild tetraploid wheat accession was reported to show no hybrid necrotic phenotype in the ABD triploid with *Net2* (Takumi and Mizuno 2011). In hybrid necrosis of higher plants, most causal genes that have been isolated to date are related to disease resistance (Bomblies et al. 2007; Alcázar et al. 2009, 2010; Yamamoto et al. 2010). Plants with type II necrosis exhibit a distinct phenotype from hybrid plants showing other types of hybrid necrosis, including marked growth suppression induced by low temperature (Mizuno et al. 2011). Arrest of cell division at the shoot apical meristem seems to occur prior to the autoimmune response in type II necrosis as well as in SGA (Mizuno et al. 2011; Hatano et al. 2012). In addition, tiller number is dramatically increased at normal temperatures in type II necrosis, although plants are significantly shorter (Takumi and Mizuno 2011). Due to these characteristics, it is still unknown which complementary genes are associated with the initial step in expression of type II necrosis.

Here, we report fine mapping of *Net2* as a step toward map-based cloning of the type II necrosis-causative gene in future studies. Recently, a draft genome sequence of *Ae. tauschii* from a whole-genome shotgun strategy was made available, which anchored 1.72 Gb of the 4.36 Gb genome to physical chromosomes (Jia et al. 2013), and a physical map of the *Ae. tauschii* genome that covers 4 Gb is available (Luo et al. 2013). In addition, barley genome information helps to efficiently assign wheat genomic and transcript sequences in silico to the barley physical map (Iehisa et al. 2012, 2014). Thus, the scaffold sequence data of the *Ae. tauschii* genome are quite useful for fine mapping of loci assigned to the D genome, such as *Iw2* and *Hch1* on 2DS and 7DS, respectively (Nishijima et al. 2014; Hirao et al. 2015). To make a fine map of the *Net2* region on 2DS, we developed *Net2*-linked markers using *Ae. tauschii* and barley genome information, and compared the chromosomal structure of the *Net2* region with the barley orthologous region based on the marker order. Moreover, to verify the usefulness of the newly developed markers around *Net2*, we analysed the genetic association of the markers closely linked to *Net2* using *Ae. tauschii* accessions that had been crossed to Ldn for phenotypic evaluation in the ABD triploids (Mizuno et al. 2010).

Materials and methods

Plant materials

Two synthetic hexaploid wheat lines generated through interspecific crosses of tetraploid wheat accession Ldn with two *Ae. tauschii* accessions, KU-2025 and KU-2075 (Mizuno et al. 2010), were used in this study. A synthetic hexaploid, Ldn/KU-2025, revealed type II necrosis (Mizuno et al. 2010), and another synthetic line, Ldn/KU-2075, showed normal growth (wild type; WT). As reported in Mizuno et al. (2010), the type II necrosis line produced

small seeds when maintained at the normal growth temperature. An F_2 mapping population was produced from crosses between Ldn/KU-2025 and Ldn/KU-2075. Seeds of the Ldn/KU-2025//Ldn/KU-2075 population were sown in November 2012, resulting in 188 F_2 individuals, which were grown in the experimental field of Kobe University. Additionally, F_3 and F_4 individuals derived from F_2 and F_3 plants heterogeneous for the *Net2* chromosomal region were respectively used for fine mapping. In the 2013–2014 season, 400 F_3 individuals of the Ldn/KU-2025//Ldn/KU-2075 population, and in the 2014–2015 season, 200 F_4 individuals were grown to increase the size of the mapping population.

Out of the *Ae. tauschii* core collection with 206 accessions, 83 were used in this study (Table S1), and their passport data, including geographical coordinates, were provided in our previous report (Matsuoka et al. 2008, 2009). Phenotypes of the 83 accessions in their ABD triploids were previously evaluated, and these accessions showed normal or type II necrosis (Mizuno et al. 2010). Previously, the 206 *Ae. tauschii* accessions were grouped into three lineages, TauL1, TauL2, and TauL3, based on DArT marker genotyping analysis (Matsuoka et al. 2013). The genotyping information on the 206 accessions was used for the 83 *Ae. tauschii* accessions for the genetic association study.

Marker development and genotyping

In our previous studies, we performed deep-sequencing analyses of the leaf and spike transcriptomes of two *Ae. tauschii* accessions, PI476874 and IG47182, that represent the two major lineages, and more than 16,000 high-confidence single nucleotide polymorphisms (SNPs) were found in 5808 contigs (Iehisa et al. 2012, 2014). The SNP information between PI476874 and IG47182 were applied to detect SNPs between Ldn/KU-2025 and Ldn/KU-2075. PI476874 and KU-2025 belong to the same lineage TauL1, and IG47182 and KU-2075 are grouped to TauL2 (Matsuoka et al. 2013). Contig sequences with the SNPs were searched with the BlastN algorithm against the *Ae. tauschii* and barley genomes (International Barley Genome Sequencing Consortium (IBSC) et al. 2012; Jia et al. 2013). These genome sequences included high-confidence genes with an *E*-value threshold of 10^{-5} and hit length $\geq$50 bp, fingerprinted contigs, and whole genome shotgun assemblies.

To choose scaffolds for *Ae. tauschii* sequences throughout the *Net2* chromosomal region, all the genes contained in each scaffold were searched with BlastN against the barley genomic sequence using the parameters described above. Scaffolds containing at least one gene aligning to the putatively corresponding region of chromosome 2HS (between 52.784 and 74.898 Mb) were considered candidates for marker development. Scaffolds without genes were anchored based on respective results from BlastN searches against the barley genome. First, high-confidence SNPs (Iehisa et al. 2012, 2014) plotted on barley 2HS were used for marker development to refine the *Net2* region. Next, SciRoKo version 3.4 software (Kofler et al. 2007) was used with the search mode setting "mismatched; fixed penalty" to identify additional simple sequence repeat (SSR) markers in sequence data of candidate scaffolds. Additional SNPs were identified in the *Net2* regions by sequencing approximately 700 bp of amplified DNA of *Ae. tauschii* accessions KU-2025 and KU-2075. The nucleotide sequences were determined using an Applied Biosystems 3730*xl* DNA Analyzer (Applied Biosystems, Foster City, CA, USA), and SNPs were found through sequence alignment using GENETYX-MAC version 12.00 software (Whitehead Institute for Biomedical Research, Cambridge, MA, USA). The identified SNPs were converted to cleaved amplified polymorphic sequence (CAPS) markers. The primer sequences for newly developed markers and any relevant restriction enzymes are listed in Table S2.

Total DNA was extracted from leaves of the parental strains and individuals of the mapping population. For SSR genotyping, 40 cycles of PCR were performed using 2× Quick Taq HS DyeMix (TOYOBO, Osaka, Japan) and the following conditions: 10 s at 94°C, 30 s at the annealing temperature, and 30 s at 68 °C. For CAPS markers, the PCR annealing temperature was 58 °C. PCR products and their digests were resolved in 2 % agarose or 13 % non-denaturing polyacrylamide gels and visualized under UV light after staining with ethidium bromide.

Construction of the 2DS linkage map

For the initial mapping of *Net2*, 188 F_2 plants were used in the Ldn/KU-2025//Ldn/KU-2075 population. Then, 400 F_3 and 200 F_4 individuals from the Ldn/KU-2025//Ldn/KU-2075 population were added for fine mapping of *Net2* with tightly linked molecular markers. The MAPMAKER/EXP version 3.0b package was used for genetic mapping (Lander et al. 1987). The threshold for log-likelihood (LOD) scores was set at 3.0, and genetic distances were calculated with the Kosambi function (Kosambi 1944).

BLAST analysis of the *Ae. tauschii* genes relative to the *Brachypodium* genome

Nucleotide sequences and annotation information for the selected *Ae. tauschii* scaffolds were analysed with reference to the *Ae. tauschii* draft genome data, which were published by Jia et al. (2013). Reference sequences from

Brachypodium (The International Brachypodium Initiative 2010) were searched against the National Center for Biotechnology Information (NCBI) NR protein database using the blastx algorithm with an *E*-value cut-off of 10^{-3}.

Association analysis of the linked markers with type II necrosis

The Q+K method was conducted using a mixed linear model function in TASSEL ver 5.0 software (Bradbury et al. 2007) for an association analysis by incorporating phenotypic and genotypic data and information on population structure. In a previous report, the Bayesian clustering approach implemented in the software program STRUCTURE 2.3 (Pritchard et al. 2000) was used with the setting $k = 2$ to predict the population structure of the *Ae. tauschii* accessions (Matsuoka et al. 2013). The Q-matrix of population membership probabilities served as covariates in the mixed linear model. Kinship (K) was calculated in TASSEL based on the genotyping information of the 169 DArT markers for the 83 *Ae. tauschii* accessions (Matsuoka et al. 2013). We performed *F* statistics and calculated the *P* values for the *F* test, and the threshold value was set as $1E^{-3}$ for a significant association. We omitted the target markers from the association analysis when their minor allele frequencies were less than 0.05.

Results and discussion

Fine mapping of *Net2* to 2DS

In the winter season, *Net2*-homozygous plants exhibited a severe growth defect and generally died in the Ldn/KU-2025//Ldn/KU-2075 F_2 population (Fig. 1). *Net2*-heterozygous plants frequently showed an intermediate phenotype of defective and delayed growth and weak necrotic symptoms. In spring, with an increase in the growth temperature, the tiller numbers increased in the *Net2*-heterozygous plants. Although the heading and flowering times were remarkably delayed compared with the *net2*-homozygous plants, selfed seeds were obtained in the *Net2*-heterozygous plants as previously reported (Mizuno et al. 2011). Based on phenotypic observation, 188 F_2 individuals segregated into 130 plants with the necrotic phenotype and 58 WT plants, fitting a 3:1 ratio ($\chi^2 = 3.433$, $P = 0.064$). Thus, type II necrosis is controlled by a single dominant allele of the *Net2* locus in the Ldn/KU-2075//Ldn/KU-2025 population. Effects of *Net2* on gamete formation and seed fertility were still unknown. The 3:1 segregation suggests no direct effects of *Net2* on the seed production-related traits.

In our previous studies, *Net2* was assigned to 2DS, and it mapped within the 8.2-cM region between an SSR (gwm102) and a SNP (HRM-10) marker (Mizuno et al. 2011; Matsuda et al. 2012). According to the available physical map information on the *Ae. tauschii* genome, 16,876 scaffolds that constitute 1.49 Gb from the draft *Ae. tauschii* genome sequence have been anchored to the linkage map of *Ae. tauschii* (Jia et al. 2013; Luo et al. 2013). The nucleotide sequences of cDNAs corresponding to the *Net2*-linked SNP markers were used as queries to select carrier scaffolds from the *Ae tauschii* sequences. We selected the *Ae tauschii* scaffolds near the *Net2*-linked marker-carrying scaffolds based on the chromosomal synteny between the wheat and barley genomes (Mayer et al. 2011; IBSC et al. 2012). In all, 55 *Ae tauschii* scaffolds were assigned in silico to an area showing synteny to the *Net2* region on the physical map of barley chromosome 2H

Fig. 2 Comparison of *Net2* linkage map, which contains *Ae. tauschii* ▶ scaffolds, with the *Ae. tauschii* linkage map and the barley physical map. The *Ae. tauschii* scaffolds were assigned to regions of the barley physical map of chromosome 2H (IBSC et al. 2012). A previously reported *Ae. tauschii* linkage map (Luo et al. 2013) is represented with the mapped scaffolds

Fig. 1 Phenotypes of segregating individuals in the Ldn/KU-2025//Ldn/KU-2075 F_2 population. *Net2*- and *Net2*-homozygous plants respectively showed WT and severe necrotic symptoms. *Net2/net2* heterozygous plants sometimes showed an intermediate phenotype, with growth inhibition and weak necrotic symptoms

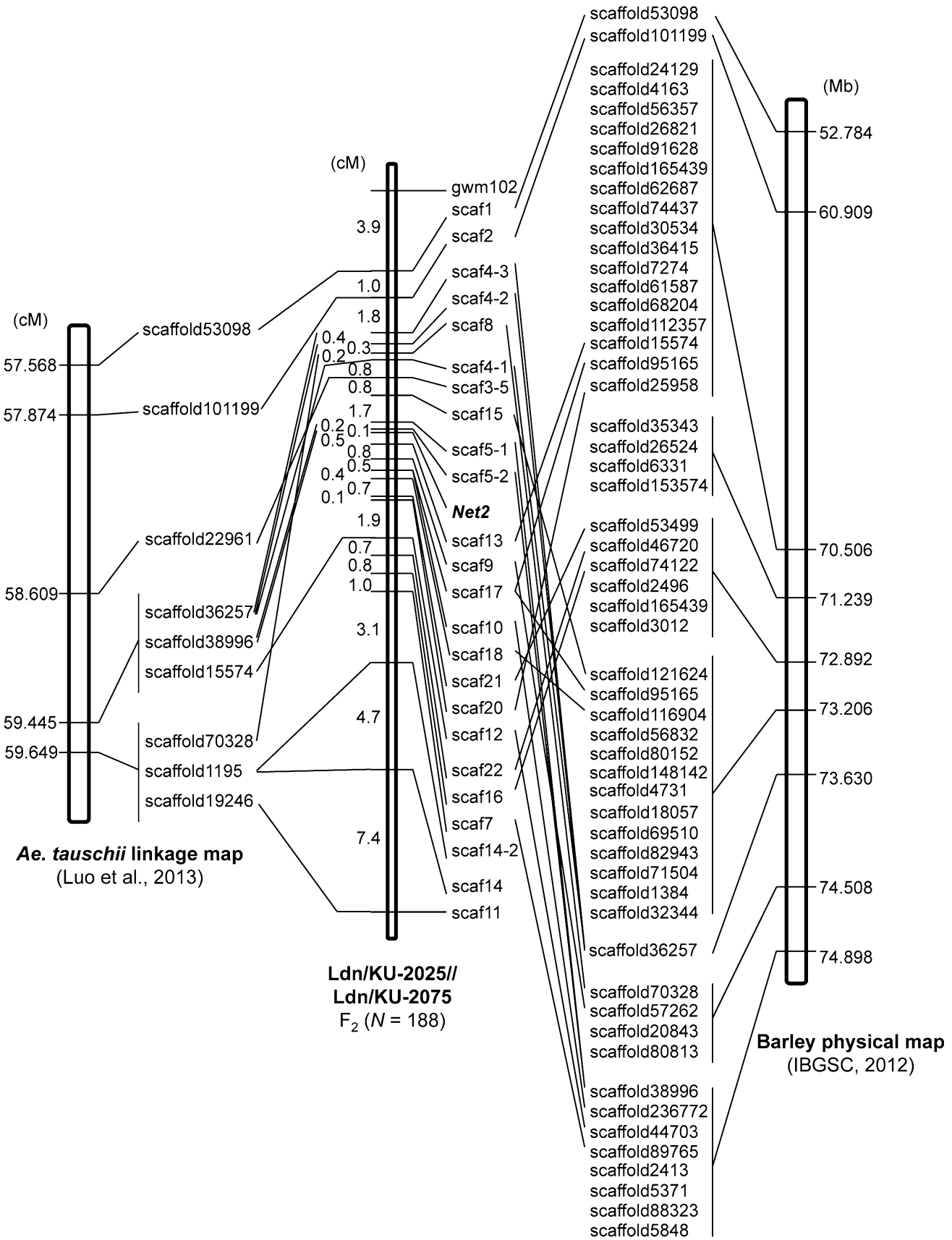
(cM)
57.568
57.874
58.609
59.445
59.649
scaffold53098
scaffold101199
scaffold22961
scaffold36257
scaffold38996
scaffold15574
scaffold70328
scaffold1195
scaffold19246
Ae. tauschii linkage map
(Luo et al., 2013)
(cM)
3.9
1.0
1.8
0.4
0.3
0.2
0.8
0.8
1.7
0.2
0.1
0.5
0.8
0.5
0.4
0.7
0.1
1.9
0.7
0.8
1.0
3.1
4.7
7.4
gwm102
scaf1
scaf2
scaf4-3
scaf4-2
scaf8
scaf4-1
scaf3-5
scaf15
scaf5-1
scaf5-2
Net2
scaf13
scaf9
scaf17
scaf10
scaf18
scaf21
scaf20
scaf12
scaf22
scaf16
scaf7
scaf14-2
scaf14
scaf11
Ldn/KU-2025//
Ldn/KU-2075
F2 (N = 188)
scaffold53098
scaffold101199
scaffold24129
scaffold4163
scaffold56357
scaffold26821
scaffold91628
scaffold165439
scaffold62687
scaffold74437
scaffold30534
scaffold36415
scaffold7274
scaffold61587
scaffold68204
scaffold112357
scaffold15574
scaffold95165
scaffold25958
scaffold35343
scaffold26524
scaffold6331
scaffold153574
scaffold53499
scaffold46720
scaffold74122
scaffold2496
scaffold165439
scaffold3012
scaffold121624
scaffold95165
scaffold116904
scaffold56832
scaffold80152
scaffold148142
scaffold4731
scaffold18057
scaffold69510
scaffold82943
scaffold71504
scaffold1384
scaffold32344
scaffold36257
scaffold70328
scaffold57262
scaffold20843
scaffold80813
scaffold38996
scaffold236772
scaffold44703
scaffold89765
scaffold2413
scaffold5371
scaffold88323
scaffold5848
(Mb)
52.784
60.909
70.506
71.239
72.892
73.206
73.630
74.508
74.898
Barley physical map
(IBGSC, 2012)

(Fig. 2). Using the 2DS linkage map of *Ae. tauschii* (Luo et al. 2013), nine *Ae tauschii* scaffolds were in silico mapped to the corresponding region on the 2DS map. Nucleotide sequences of the selected scaffolds were used to design CAPS or SSR markers for each scaffold, and the markers were mapped in the F_2 population after their polymorphisms were confirmed between the parental synthetic hexaploids Ldn/KU-2025 and Ldn/KU-2075. In the selected scaffolds, 510 SSR and 99 SNP markers were designed, and polymorphisms between the parental lines were found in 20 SSR and eight SNP markers.

Using 24 of the polymorphic markers, 20 of the selected *Ae tauschii* scaffolds were anchored to the *Net2* chromosomal region (Fig. 2; Table S2). No polymorphisms between Ldn/KU-2025 and Ldn/KU-2075 were found in the remaining scaffolds. In the Ldn/KU-2025//Ldn/KU-2075 population with 188 F_2 individuals, the *Net2* locus was mapped within a 0.6 cM interval between the linked marker scaf5-2, derived from scaffold 38996, and scaf13, from scaffold 15574. Next, the *Net2* locus was mapped together with 11 co-dominant markers in 788 individuals of the Ldn/KU-2025//Ldn/KU-2075 population to construct the *Net2* fine map (Fig. 3). The 788 individuals were segregated into 602 plants with the necrotic phenotype and 186 WT plants, fitting a 3:1 ratio ($\chi^2 = 0.819$, $P = 0.365$). On the fine map, *Net2* was located within the 1.6 cM interval between scaf5-2 and scaf13. There were nine recombinants among the 788 individuals for the markers. In the *Ae. tauschii* linkage map (Luo et al. 2013), the scaffolds 38996 and 15574 co-localized to the 59.445-cM position of 2DS (Fig. 2). These observations suggest that *Net2* is localized near scaffolds 38996 and 15574 or within one of them on 2DS. The scaffolds 38996 and 15574 were respectively 130.4 and 88.1 kb in length (Fig. 3), whereas the gap length between them is unknown. Construction of a bacterial artificial chromosome contig covering the *Net2* region will be required for further studies toward map-based cloning of *Net2*.

Chromosomal synteny in the *Net2* region among related species

The markers mapping near *Net2* in the 188 F_2 individuals covered the 57.568–59.649 cM chromosomal region in the *Ae. tauschii* genome (Fig. 2). This *Net2* chromosomal region corresponded to the 52.784–74.898 Mb region on 2HS of the barley genome. Scaffold 38996 was located at the 74.898 Mb position, whereas scaffold 15574 was at the 70.506 Mb site in the *Net2*-corresponding chromosomal region. The order of the *Net2*-linked markers on the *Ae. tauschii* 2DS map was not necessarily conserved in the corresponding region of the barley 2HS physical map (Fig. 2). These observations indicate that complicated rearrangements occurred in the chromosomal region containing *Net2* during the divergence between barley and *Ae. tauschii*. Similar rearrangements such as inversions have been reported in the chromosomal regions for *Iw2*, a wax inhibitor on 2DS, and *Hch1*, controlling hybrid chlorosis on 7DS, between the barley and *Ae. tauschii* genomes (Nishijima et al. 2014; Hirao et al. 2015). Chromosomal synteny was generally well conserved on each chromosome arm between the barley and *Ae. tauschii* genomes, as previously reported (Mayer et al. 2011). However, a lot of minor rearrangements likely accumulated locally after divergence of the diploid genomes in the tribe Triticeae.

Fig. 3 Comparison of *Ae. tauschii* linakge map of the *Net2* region with 788 individuals, the scaffolds, and *Brachypodium* chromosomes. The nine *Ae. tauschii* scaffolds, shown with gene and contig numbers, were putatively anchored to the *Net2* region. Positions of the *Net2*-linked markers on the nine scaffolds are shown by the *connected lines*. The regions orthologous to *Net2* on *Brachypodium* chromosomes with gene models are represented, and orthologous relationships are indicated by the *connected lines*

The 11 markers used for the *Net2* fine mapping were derived from the nine *Ae. tauschii* scaffolds. Each of the scaffolds was 30.8–130.4 kb and contained one to eight protein-coding genes (Jia et al. 2013; Luo et al. 2013). Thirty genes, including 24 with an AEGTA number and six contigs, appeared on the nine scaffolds (Fig. 3). Scaffolds 38996 and 15574 contained eight and two genes, respectively. The *Ae. tauschii* scaffolds that included protein-coding genes were used as queries to search the *Brachypodium* genomic information by a BlastN search. Putative orthologs of the *Ae. tauschii* genes from the nine scaffolds were mainly assigned to chromosome 1 of *Brachypodium* (Fig. 3). One gene in scaffold 38996 was orthologous to genes assigned to chromosome 2, and some paralogous copies to AEGTA15710 in scaffold 74122 were distributed to chromosomes 1–5. With these exceptions, the *Net2* region on 2DS showed chromosomal synteny to the broad region of *Brachypodium* chromosome 1. In spite of some small inversions, translocations and duplications, the gene order was generally conserved during divergence between *Brachypodium* and *Ae. tauschii*.

Hybrid necrosis is widely known to be triggered by autoimmune responses due to epistatic interaction of disease resistance-related genes in higher plants (Bomblies et al. 2007; Alcázar et al. 2009, 2010; Yamamoto et al. 2010). Of the 18 *Ae. tauschii* genes in the four scaffolds near *Net2*, 10 (8 AEGTAs and 2 contigs) had obvious orthologs in the *Brachypodium* genome (Table 1). However, three AEGTA genes were putatively orthologous to *Brachypodium* genes encoding GDSL-like lipase protein or ARM repeat protein in the *Net2*-linked scaffolds 38996 and 15774, and thus no apparent NB-LRR-type resistance

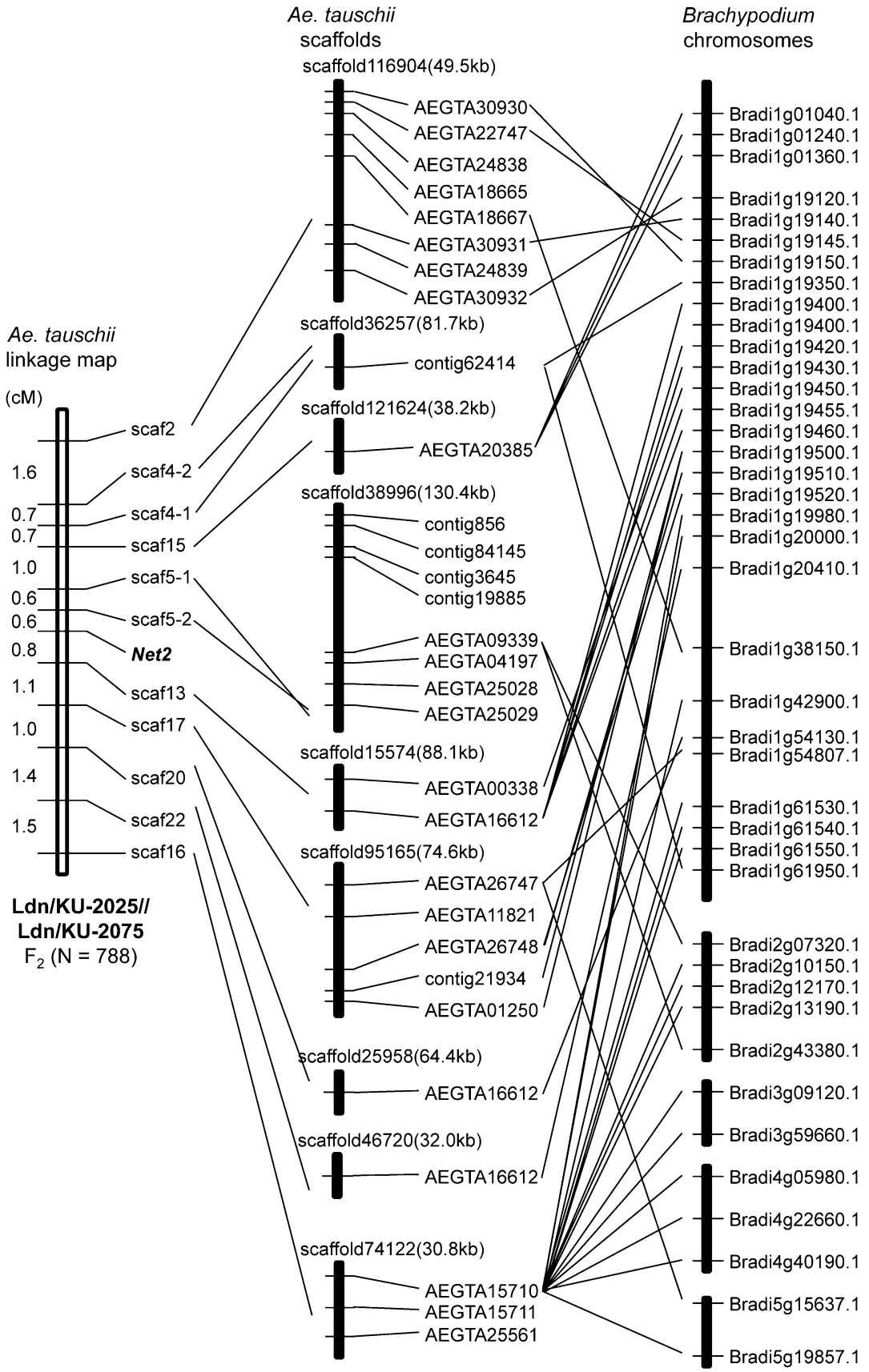
Ae. tauschii
scaffolds
Brachypodium
chromosomes
Ae. tauschii
linkage map
(cM)
scaf2
1.6
scaf4-2
0.7
scaf4-1
0.7
scaf15
1.0
scaf5-1
0.6
scaf5-2
0.6
Net2
0.8
scaf13
1.1
scaf17
1.0
scaf20
1.4
scaf22
1.5
scaf16
Ldn/KU-2025//
Ldn/KU-2075
F2 (N = 788)
scaffold116904(49.5kb)
AEGTA30930
AEGTA22747
AEGTA24838
AEGTA18665
AEGTA18667
AEGTA30931
AEGTA24839
AEGTA30932
scaffold36257(81.7kb)
contig62414
scaffold121624(38.2kb)
AEGTA20385
scaffold38996(130.4kb)
contig856
contig84145
contig3645
contig19885
AEGTA09339
AEGTA04197
AEGTA25028
AEGTA25029
scaffold15574(88.1kb)
AEGTA00338
AEGTA16612
scaffold95165(74.6kb)
AEGTA26747
AEGTA11821
AEGTA26748
contig21934
AEGTA01250
scaffold25958(64.4kb)
AEGTA16612
scaffold46720(32.0kb)
AEGTA16612
scaffold74122(30.8kb)
AEGTA15710
AEGTA15711
AEGTA25561
Bradi1g01040.1
Bradi1g01240.1
Bradi1g01360.1
Bradi1g19120.1
Bradi1g19140.1
Bradi1g19145.1
Bradi1g19150.1
Bradi1g19350.1
Bradi1g19400.1
Bradi1g19400.1
Bradi1g19420.1
Bradi1g19430.1
Bradi1g19450.1
Bradi1g19455.1
Bradi1g19460.1
Bradi1g19500.1
Bradi1g19510.1
Bradi1g19520.1
Bradi1g19980.1
Bradi1g20000.1
Bradi1g20410.1
Bradi1g38150.1
Bradi1g42900.1
Bradi1g54130.1
Bradi1g54807.1
Bradi1g61530.1
Bradi1g61540.1
Bradi1g61550.1
Bradi1g61950.1
Bradi2g07320.1
Bradi2g10150.1
Bradi2g12170.1
Bradi2g13190.1
Bradi2g43380.1
Bradi3g09120.1
Bradi3g59660.1
Bradi4g05980.1
Bradi4g22660.1
Bradi4g40190.1
Bradi5g15637.1
Bradi5g19857.1

genes were present. In addition to autoimmune responses, arrest of cell division has been observed at shoot apical meristems with the type II necrosis phenotype under low temperature (Mizuno et al. 2011). Suppression of cell cycle-related gene expression inhibits plant growth and induces necrotic cell death in *Arabidopsis* (Wang and Liu 2006; Lin et al. 2007). Therefore, *Net2* might be related to the cell cycle and cell division rather than disease resistance. To clarify the initial gene interaction resulting in type II necrosis, the molecular nature of *Net2* should first be elucidated.

Genetic association of the *Net2*-linked markers with type II necrosis

To determine the genetic association between developed markers and type II necrosis, 12 *Net2*-linked PCR markers including 11 SSRs and one CAPS were used to genotype the 83 *Ae. tauschii* accessions (Table S1). Of the 83 accessions, 22 showed type II necrosis in ABD triploid hybrids after crossing to Ldn, and 61 produced WT synthetic hexaploids. Most of the accessions showing type II necrosis belong to the TauL1b sublineage, dispersed in eastern habitats in the *Ae. tauschii* population (Matsuoka et al. 2013; Table S1). The restricted distribution suggests that the *Net2* dominant allele might be derived from one mutation in the original *net2* recessive allele. All 12 markers exhibited just two apparent alleles, the KU-2075 type and KU-2025 type. No obvious marker in which the genotype completely corresponded to the WT/type II necrosis phenotypes was found in the examined 12 markers (Table 2).

Out of the 12 *Net2*-linked markers, three SSRs, scaf8, scaf5-1 and scaf5-2 and one CAPS marker, scaf13, were significantly ($P < 1E^{-3}$) associated with the WT/type II necrosis phenotypic difference (Fig. 4). Three associated markers, scaf5-1, scaf5-2 and scaf13, were the most closely linked to *Net2*, whereas the scaf8 marker was slightly further from the three markers and *Net2*. At the scaf5-2 marker with the lowest *P* value, six of the 61 WT accessions showed the KU-2025-type allele and seven of the 22 type II necrosis accessions carried the KU-2075-type allele. Therefore, the chromosomal region around scaffolds 38996 and 15574 were highly associated with the WT/type II necrosis phenotypic difference, meaning that *Net2* should be localized in this region. These results suggest that the three PCR markers derived from the two scaffolds will be efficient for selection of *Net2* non-carrier individuals from the *Ae. tauschii* population and its intraspecific progeny. The eastern habitat accessions of *Ae. tauschii* provide useful genes for breeding of the D genome of common wheat (Kajimura et al. 2011; Jones et al. 2013), and many of them contain *Net2* (Mizuno et al. 2010). Thus, these

Table 1 Colinearity between *Ae. tauschii* and *Brachypodium* in the syntenic genomic regions around *Net2*

Scaffold in *Ae. tauschii*	*Ae. tauschii* putative gene	*Brachypodium* gene	Annotation
scaffold36257	contig62414	Bradi1g19350.1	Tetratricopeptide repeat (TPR)-like protein
		Bradi1g61950.1	Tetratricopeptide repeat (TPR)-like protein
scaffold121624	AEGTA20385	Bradi1g01040.1	Heat shock protein 101
		Bradi1g01360.1	Heat shock protein 101
		Bradi1g01240.1	Heat shock protein 101
scaffold38996	AEGTA09339	Bradi2g43380.1	GDSL-like lipase/acylhydrolase
		Bradi2g07320.1	GDSL-like lipase/acylhydrolase
scaffold15574	AEGTA00338	Bradi1g19450.1	ARM repeat protein
	AEGTA16612	Bradi1g19460.1	ARM repeat protein
		Bradi1g19420.1	ARM repeat protein
		Bradi1g19430.1	ARM repeat protein
		Bradi1g19455.1	ARM repeat protein
		Bradi1g19400.1	ARM repeat protein
scaffold95165	AEGTA01250	Bradi1g19500.1	P-loop containing nucleoside triphosphate hydrolases
	AEGTA26747	Bradi1g54807.1	RNA ligase
		Bradi5g15637.1	RNA ligase
	AEGTA26748	Bradi1g19510.1	E3 Ubiquitin ligase
		Bradi1g19520.1	Unknown
	contig21934	Bradi1g19500.1	P-loop containing nucleoside triphosphate hydrolases
scaffold25958	AEGTA14976	Bradi2g51530.1	Cytokinin oxidase 5

Table 2 Association between *Net2*-linked marker genotypes and WT versus type II necrosis phenotypes in 83 accessions of *Ae. tauschii*

Marker name	Marker type	WT (N = 61)		Type II necrosis (N = 22)	
		KU-2075 type (WT)	KU-2025 type (type II necrosis)	KU-2075 type (WT)	KU-2025 type (type II necrosis)
scaf1	SSR	34	27	0	22
scaf2	SSR	45	16	12	10
scaf4-2	SSR	8	53	0	22
scaf8	SSR	24	37	17	5
scaf4-1	SSR	60	1	22	0
scaf3-5	SSR	24	37	0	22
scaf15	SSR	37	24	9	13
scaf5-1	SSR	51	10	9	13
scaf5-2	SSR	55	6	7	15
scaf13	CAPS	55	6	6	16
scaf9	SSR	49	12	5	17
scaf17	SSR	38	23	0	22

The numbers of accessions for each genotype are represented in WT and type II necrosis phenotypes in the ABD triploids

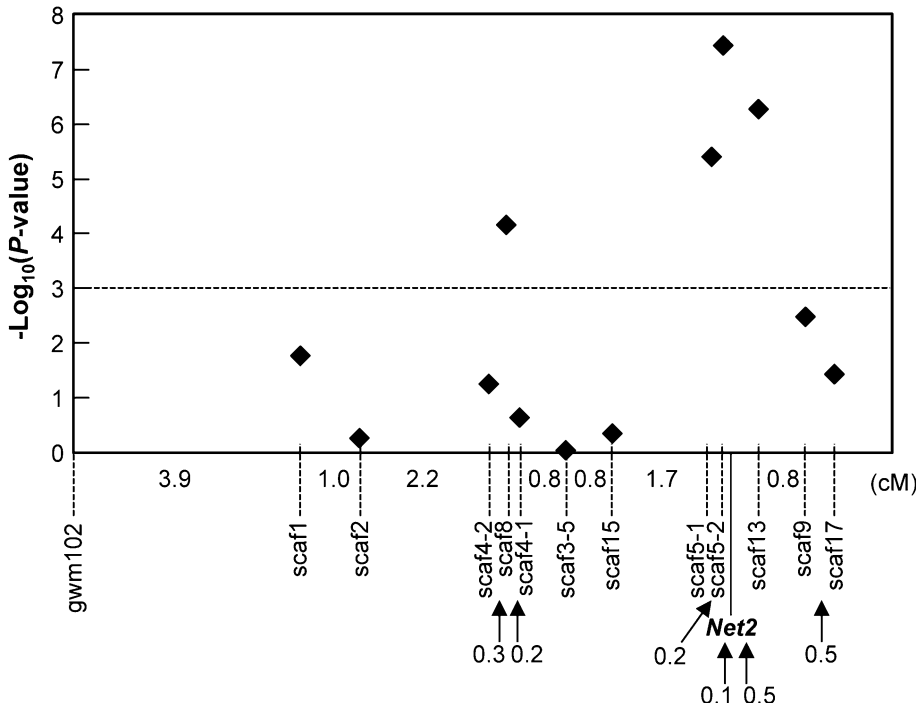

Fig. 4 Trait associations with marker polymorphisms at the *Net2* locus. *The horizontal axis* represents the position of each examined marker in the linkage map ($N = 188$). The $-\log(P$ value) values were calculated based on a mixed linear model in TASSEL ver. 4.0 software. The threshold for significance ($P < 1E^{-3}$) is indicated by the *dashed line*

markers could help the introgression of agriculturally important genes from *Ae. tauschii* to common wheat.

Conclusion

Net2, the causal gene for low-temperature induced hybrid necrosis, inhibits efficient use of *Ae. tauschii* for the D-genome breeding of common wheat. In the present study, the *Net2* locus, the D-genome causal gene for type II necrosis, was mapped within the 0.6-cM region on 2DS of synthetic hexaploid wheat. The most closely linked markers also showed highly significant association with the WT/type II necrosis phenotype in *Ae. tauschii*. Although local chromosomal rearrangements were observed in the region corresponding to *Net2* in comparison of the barley/*Brachypodium* and *Ae. tauschii* genomes, our results provide useful information toward map-based cloning of *Net2*. On the other hand, the number of scaffolds assigned to the *Net2* region was higher in the barley physical map than in

the *Ae. tauschii* linkage map. In the draft genome sequence of *Ae. tauschii*, many scaffolds have failed to be positioned to chromosomes (Jia et al. 2013; Luo et al. 2013; Iehisa et al. 2012, 2014). In addition, the lowest *P* values in the association study for *Net2* was much higher than the values for *Iw2* on 2DS (Nishijima et al. 2014). These observations imply the possible existence of additional scaffolds that failed in assignments to the *Net2* region in this study. Updated information for the diploid and polyploid wheat genome sequences using assemblies with NRGene's DeNovoMAGIC software (https://wheat-urgi.versailles.inra.fr) could be useful for the additional detection of scaffolds around *Net2*. A recent report showed that bulked segregant analysis using next generation sequencing technology is effective in identifying molecular markers tightly linked to target loci (Borrill et al. 2015). Thus, RNA sequencing-based bulked segregant analysis could be efficient for discovery of additional unanchored *Ae. tauschii* scaffolds in the *Net2* region.

Acknowledgments We thank Dr. Yoshihiro Matsuoka for his providing of the genotyping data of the 83 *Ae. tauschii* accessions and Dr. Kentaro Yoshida for his critical reading of the manuscript. This work was supported by grants from the Ministry of Education, Culture, Sports, Science and Technology (MEXT) of Japan (Grant-in-Aid for Scientific Research (B) Nos. 25292008 and 16H04862).

References

Alcázar R, García AV, Parker JE, Reymond M (2009) Incremental steps toward incompatibility revealed by Arabidopsis epistatic interactions modulating salicylic acid pathway activation. Proc Natl Acad Sci USA 106:334–339

Alcázar R, García AV, Kronholm I, de Meaux J, Koornneef M, Parker JE, Reymond M (2010) Natural variation at Strubbelig Receptor Kinase 3 drives immune-triggered incompatibilities between *Arabidopsis thaliana* accessions. Nat Genet 42:1135–1139

Bomblies K, Lempe J, Epple P, Warthmann N, Lanz C, Dangl JL, Weigel D (2007) Autoimmune response as a mechanism for Dobzhansky-Muller-type incompatibility syndrome in plants. PLoS Biol 5:e236

Borrill P, Adamski N, Uauy C (2015) Genomics as the key to unlocking the polyploid potential of wheat. New Phytol 208:1008–1022

Bradbury PJ, Zhang Z, Kroon DE, Casstevens TM, Ramdoss Y, Buckler ES (2007) TASSEL: software for association mapping of complex traits in diverse samples. Bioinformatics 23:2633–2635

Chu CG, Faris JD, Friesen TL, Xu SS (2006) Molecular mapping of hybrid necrosis genes *Ne1* and *Ne2* in hexaploid wheat using microsatellite markers. Theor Appl Genet 112:1374–1381

Dvorak J, Luo MC, Yang ZL, Zhang HB (1998) The structure of the *Aegilops tauschii* genepool and the evolution of hexaploid wheat. Theor Appl Genet 97:657–670

Hatano H, Mizuno N, Matsuda R, Shitsukawa N, Park P, Takumi S (2012) Dysfunction of mitotic cell division at shoot apices triggered severe growth abortion in interspecific hybrids between tetraploid wheat and *Aegilops tauschii*. New Phytol 194:1143–1154

Hirao K, Nishijima R, Sakaguchi K, Takumi S (2015) Fine mapping of *Hch1*, the causal D-genome gene for hybrid chlorosis in interspecific crosses between tetraploid wheat and *Aegilops tauschii*. Genes Genet Syst 90:283–291

Iehisa JCM, Shimizu A, Sato K, Nasuda S, Takumi S (2012) Discovery of high-confidence single nucleotide polymorphisms from large-scale de novo analysis of leaf transcripts of *Aegilops tauschii*, a wild wheat progenitor. DNA Res 19:487–497

Iehisa JCM, Shimizu A, Sato K, Nishijima R, Sakaguchi K, Matsuda R, Nasuda S, Takumi S (2014) Genome-wide marker development for the wheat D genome based on single nucleotide polymorphisms identified from transcripts in the wild wheat progenitor *Aegilops tauschii*. Theor Appl Genet 127:261–271

International Barley Genome Sequencing Consortium, Mayer KF, Waugh R, Brown JW, Schulman A, Langridge P, Platzer M, Fincher GB, Muehlbauer GJ, Sato K, Close TJ, Wise RP, Stein N (2012) A physical, genetic and functional sequence assembly of the barley genome. Nature 491:711–716

Jia J, Zhao S, Kong X, Li Y, Zhao G, He W, Appels R, Pfeifer M, Tao Y, Zhang X, Jing R, Zhang C, Ma Y, Gao L, Gao C, Spannagl M, Mayer KFX, Li D, Pan S, Zheng F, Hu Q, Xia X, Li J, Liang Q, Chen J, Wicker T, Gou C, Kuang H, He G, Luo Y, Keller B, Xia Q, Lu P, Wang J, Zou H, Zhang R, Gao J, Middleton C, Quan Z, Liu G, Wang J, International Wheat Genome Sequencing Consortium, Yang H, Liu X, He Z, Mao L, Wang J (2013) *Aegilops tauschii* draft genome sequence reveals a gene repertoire for wheat adaptation. Nature 496:91–95

Jones H, Gosman N, Horsnell R, Rose GA, Everest LA, Bentley AR, Tha S, Uauy C, Kowalski A, Novoselovic N, Simek R, Kobiljski B, Kondic-Spika A, Brbaklic L, Mitrofanova O, Chesnokov Y, Bonnett D, Greenland A (2013) Strategy for exploiting exotic germplasm using genetic, morphological, and environmental diversity: the *Aegilops tauschii* Coss. example. Theor Appl Genet 126:1793–1808

Kajimura T, Murai K, Takumi S (2011) Distinct genetic regulation of flowering time and grain-filling period based on empirical study of D-genome diversity in synthetic hexaploid wheat lines. Breed Sci 61:130–141

Kihara H, Lilienfeld F (1949) A new synthesized 6x-wheat. Hereditas (Supplemental Volume):307–319

Kofler R, Schlötterer C, Lelley T (2007) SciRoKo: a new tool for whole genome microsatellite search and investigation. Bioinformatics 23:1683–1685

Kosambi DD (1944) The estimation of map distance from recombination values. Ann Eugen 12:172–175

Lander ES, Green P, Abrahamson J (1987) MAPMAKER: an interactive computer package for constructing primary genetic linkage maps of experimental and natural populations. Genomics 1:174–181

Lin Z, Yin K, Zhu D, Chen Z, Gu H, Qu LJ (2007) AtCDC5 regulates the G2 to M transition of the cell cycle and is critical for the function of *Arabidopsis* shoot apical meristem. Cell Res 17:815–828

Luo MC, Gu YQ, You FM, Deal KR, Ma Y, Hu Y, Huo N, Wang Y, Wang J, Chen S, Jorgensen CM, Zhang Y, McGuire PE, Pasternak S, Stein JC, Ware D, Kramer M, McCombie WR, Kianian SF, Martis MM, Mayer KFX, Sehgal SK, Li W, Gill BS, Bevan MW, Šimková H, Doležel J, Weining S, Lazo GR, Anderson OD, Dvorak J (2013) A 4-gigabase physical map unlocks the structure and evolution of the complex genome of *Aegilops tauschii*, the wheat D-genome progenitor. Proc Natl Acad Sci USA 110:7940–7945

Matsuda R, Iehisa JCM, Takumi S (2012) Application of real-time PCR-based SNP detection for mapping of *Net2*, a causal D-genome gene for hybrid necrosis in interspecific crosses

between tetraploid wheat and *Aegilops tauschii*. Gene Genet Syst 87:137–143

Matsuoka Y (2011) Evolution of polyploid *Triticum* wheats under cultivation: the role of domestication, natural hybridization and allopolyploid speciation in their diversification. Plant Cell Physiol 52:750–764

Matsuoka Y, Nasuda S (2004) Durum wheat as a candidate for the unknown female progenitor of bread wheat: an empirical study with a highly fertile F_1 hybrid with *Aegilops tauschii* Coss. Theor Appl Genet 109:1710–1717

Matsuoka Y, Takumi S, Kawahara T (2007) Natural variation for fertile triploid F_1 formation in allohexaploid wheat speciation. Theor Appl Genet 115:509–518

Matsuoka Y, Takumi S, Kawahara T (2008) Flowering time diversification and dispersal in central Eurasian wild wheat *Aegilops tauschii* Coss.: genealogical and ecological framework. PLoS ONE 3:e3138

Matsuoka Y, Nishioka E, Kawahara T, Takumi S (2009) Genealogical analysis of subspecies divergence and spikelet-shape diversification in Central Eurasian wild wheat *Aegilops tauschii* Coss. Plant Syst Evol 279:233–244

Matsuoka Y, Nasuda S, Ashida Y, Nitta M, Tsujimoto H, Takumi S, Kawahara T (2013) Genetic basis for spontaneous hybrid genome doubling during allopolyploid speciation of common wheat shown by natural variation analyses of the paternal species. PLoS ONE 8:e68310

Mayer KFX, Martis M, Hedley PE, Simkova H, Liu H, Morris JA, Steuernagel B, Taudien S, Roesner S, Gundlach H, Kubaláková M, Suchánková P, Murat F, Felder M, Nussbaumer T, Graner A, Salse J, Endo T, Sakai H, Tanaka T, Itoh T, Sato K, Platzer M, Matsumoto T, Scholz U, Dolezel J, Waugh R, Stein N (2011) Unlocking the barley genome by chromosomal and comparative genomics. Plant Cell 23:1249–1263

Mizuno N, Hosogi N, Park P, Takumi S (2010) Hypersensitive response-like reaction is associated with hybrid necrosis in interspecific crosses between tetraploid wheat and *Aegilops tauschii* Coss. PLoS ONE 5:e11326

Mizuno N, Shitsukawa N, Hosogi N, Park P, Takumi S (2011) Autoimmune response and repression of mitotic cell division occur in inter-specific crosses between tetraploid wheat and *Aegilops tauschii* Coss. that show low temperature-induced hybrid necrosis. Plant J 68:114–128

Mujeeb-Kazi A, Rosas V, Roldan S (1996) Conservation of the genetic variation of *Triticum tauschii* (Coss.) Schmalh. (*Aegilops squarrosa* auct. non L.) in synthetic hexaploid wheats (*Triticum turgidum* L. s.lat. x *T. tauschii*; $2n = 6x = 42$, AABBDD) and its potential utilization for wheat improvement. Genet Res Crop Evol 43:129–134

Nakano H, Mizuno N, Tosa Y, Yoshida K, Park P, Takumi S (2015) Accelerated senescence and enhanced disease resistance in hybrid chlorosis lines derived from interspecific crosses between tetraploid wheat and *Aegilops tauschii*. PLoS ONE 10:e0121583

Nishijima R, Iehisa JCM, Matsuoka Y, Takumi S (2014) The cuticular wax inhibitor locus *Iw2* in wild diploid wheat *Aegilops tauschii*: phenotypic survey, genetic analysis, and implications for the evolution of common wheat. BMC Plant Biol 14:246

Nishikawa K (1960) Hybrid lethality in crosses between emmer wheats and *Aegilops squarrosa*, I. Vitality of F_1 hybrids between emmer wheats and *Ae. squarrosa* var. *typica*. Seiken Ziho 11:21–28

Nishikawa K (1962) Hybrid lethality in crosses between emmer wheats and *Aegilops squarrosa*, III. Gene analysis of type-2 necrosis. Seiken Ziho 14:45–50

Pritchard JK, Stephens M, Donnelly P (2000) Inference of population structure using multilocus genotype data. Genetics 155:945–959

Takumi S, Mizuno N (2011) Low temperature-induced necrosis shows phenotypic plasticity in wheat triploid hybrids. Plant Signal Behav 6:1431–1433

Takumi S, Nishioka E, Morihiro H, Kawahara T, Matsuoka Y (2009) Natural variation of morphological traits in wild wheat progenitor *Aegilops tauschii* Coss. Breed Sci 59:579–588

The International Brachypodium Initiative (2010) Genome sequencing and analysis of the model grass *Brachypodium distachyon*. Nature 463:763–768

Tsunewaki K (1960) Monosomic and conventional gene analysis in common wheat. III. Lethality. Jpn J Genet 35:594–601

Tsunewaki K (1966) Comparative gene analysis of common wheat and its ancestral species. II. Waxiness, growth habit and awnedness. Jpn J Bot 19:175–229

Wang C, Liu Z (2006) *Arabidopsis* ribonucleotide reductases are critical for cell cycle progression, DNA damage repair, and plant development. Plant Cell 18:350–365

Wang J, Luo MC, Chen Z, You FM, Wei Y, Zheng Y, Dvorak J (2013) *Aegilops tauschii* single nucleotide polymorphisms shed light on the origins of wheat D-genome genetic diversity and pinpoint the geographic origin of hexaploid wheat. New Phytol 198:925–937

Yamamoto E, Takashi T, Morinaka Y, Lin S, Wu J, Matsumoto T, Kitano H, Matsuoka M, Ashikari M (2010) Gain of deleterious function caused an autoimmune response and Bateson–Dobzhansky–Muller incompatibility in rice. Mol Genet Genomics 283:305–315

Zhang P, Hiebert CW, McIntosh RA, McCallum BD, Thomas JB, Hoxha S, Singh D, Bansal U (2016) The relationship of leaf rust resistance gene *Lr13* and hybrid necrosis gene *Ne2m* on wheat chromosome 2BS. Theor Appl Genet 129:485–493